# Assessment and prediction of thermal transport at solid–self-assembled monolayer junctions

John C. Duda, Christopher B. Saltonstall, Pamela M. Norris, and Patrick E. Hopkins

Citation: J. Chem. Phys. **134**, 094704 (2011); doi: 10.1063/1.3557823
View online: http://dx.doi.org/10.1063/1.3557823
View Table of Contents: http://jcp.aip.org/resource/1/JCPSA6/v134/i9
Published by the American Institute of Physics.

# Assessment and prediction of thermal transport at solid–self-assembled monolayer junctions

John C. Duda,[1,2,a)] Christopher B. Saltonstall,[1,b)] Pamela M. Norris,[1,c)] and Patrick E. Hopkins[1,2,d)]
[1]*Department of Mechanical and Aerospace Engineering, University of Virginia, Charlottesville, Virginia 22904, USA*
[2]*Engineering Sciences Center, Sandia National Laboratories, Albuquerque, New Mexico 87185, USA*

(Received 10 October 2010; accepted 2 February 2011; published online 2 March 2011; publisher error corrected 8 March 2011)

Self-assembled monolayers (SAMs) have recently garnered much interest due to their unique electrical, chemical, and thermal properties. Several studies have focused on thermal transport across solid–SAM junctions, demonstrating that interface conductance is largely insensitive to changes in SAM length. In the present study, we have investigated the vibrational spectra of alkanedithiol-based SAMs as a function of the number of methylene groups forming the molecular backbone via Hartree–Fock methods. In the case of Au–alkanedithiol junctions, it is found that despite the addition of nine new vibrational modes per added methylene group, only one of these modes falls below the maximum phonon frequency of Au. In addition, the alkanedithiol one-dimensional density of normal modes (modes per unit energy per unit length) is nearly constant regardless of chain length, explaining the observed insensitivity. Furthermore, we developed a diffusive transport model intended to predict interface conductance at solid–SAM junctions. It is shown that this predictive model is in an excellent agreement with prior experimental data available in the literature. © *2011 American Institute of Physics*. [doi:10.1063/1.3557823]

## I. INTRODUCTION

Self-assembled monolayers (SAMs) are thin layers of molecules that arrange themselves in an aligned array on the substrate on which they are deposited. Such monolayers are often comprised of linear alkanes, silanes, or benzenes ranging from a few to tens of angstroms long. Each molecule can be further functionalized via end groups such that a particular property of the molecule is enhanced or inhibited (e.g., hydrophilicity or hydrophobicity). Self-assembled monolayers have recently garnered much interest due to the combination of their unique electrical, chemical, and thermal properties. Specifically, SAMs and solid–SAM junctions have shown promise in the fields of molecular electronics,[1] thermoelectric power generation and cooling,[2] chemical functionalization of interfaces,[3–5] and thermal rectification.[5,6]

The need for thermal characterization of these molecules and the interfaces they comprise depends largely on the particular application for which the material system is suited. In the case of thermoelectricity, the dimensionless figure of merit is inversely proportional to effective thermal conductivity. As for thermal rectification, the degree of rectification is related to the efficiency of thermal transport in one-direction relative to that in the opposite direction. Within the field of molecular electronics, this emphasis on thermal transport has been driven in part by the findings of Segal and Nitzin,[7] who demonstrated that as much as 50% of the voltage drop across a molecule will be dissipated as heat, thus suggesting that the efficiency of heat conduction away from the junction will be a critical factor affecting related applications.

Explicit experimental thermal characterization of solid–SAM interfaces has been fairly limited. Both Wilson *et al.*[3] and Ge *et al.*[4] indirectly investigated such interfaces by focusing instead on solid–SAM–liquid interfaces. Wilson *et al.*[3] used subpicosecond laser pulses to study transient absorption and thermal transport between alkanethiol-stabilized metallic nanoparticles and a surrounding fluid matrix. In this particular study, it was found that the efficiency of thermal transport exhibited a larger dependence on the surrounding matrix ($H_2O$ or toluene) rather than the particular stabilizing molecule implemented. Ge *et al.*[4] used time-domain thermoreflectance to study thermal transport across planar interfaces between alkanethiol-functionalized metals and water, finding that the particular functionalization (hydrophobic or hydrophilic) could change the efficiency of thermal transport across the interface by a factor of 2.

Turning to the studies which focused specifically on solid–SAM interface conductance, Wang *et al.*[8] measured the thermal conductance of Au–SAM–GaAs sandwiches via the $3\omega$ technique, where the SAM was comprised of alkanedithiols eight, nine, or ten methylene groups long. It was found that the conductance of these composite junctions was insensitive to changes in the length of the alkanedithiols. However, due to the asymmetry of the junction, the authors did not speculate on the efficiency of thermal transport at an individual solid–SAM interface. Wang *et al.*[9,10] used sum-frequency generation (SFG) spectroscopy to measure the ultrafast thermal conductance across Au–SAM (alkanethiol and benzenethiol) junctions. These studies once again found that thermal conductance measurements were insensitive to the

a)Electronic mail: duda@virginia.edu.
b)Electronic mail: cbs4b@virginia.edu.
c)Electronic mail: pamela@virginia.edu.
d)Electronic mail: pehopki@sandia.gov.

 

length of the molecules forming the SAM, indicative of interface-limited thermal transport.[9,10] The authors reported interface conductance to be $220 \pm 100$ MW m$^{-2}$ K$^{-1}$ at 1000 K. This value is higher than others reported in the literature due to the ultrafast nature of the imparted heat pulses and subsequent measurement.

Computational characterization of SAMs has been split largely into two categories: works those focusing on single molecules and works those focusing on solid–SAM junctions. Segal and Nitzan have used classical[7] and quantum mechanical[6,11] models to investigate thermal transport in single molecules coupled to external baths. Of particular interest is the fact that molecular thermal conductance (along a molecule, not across a junction) of alkanes was found to be insensitive to changes in chain length for alkanes seven or more methylene groups long.[11] Additionally, it was noted that anharmonic interactions within the molecule were relatively small (<1%). This finding suggests that it is safe to assume these (alkanes) and similar molecular chains behave harmonically.

Luo and Lloyd performed both equilibrium[12] and nonequilibrium[13] molecular dynamics studies of thermal transport across Au–SAM–Au sandwiches. In the equilibrium work,[12] SAMs were comprised of alkanedithiols ranging from eight to ten methylene groups long. It was found that the predicted thermal conductance of Au–SAM–Au junctions was only weakly, if at all, sensitive to changes in molecule chain length. It was subsequently suggested that this observed behavior could be attributed to the Au–SAM interfaces ultimately dictating the efficiency of thermal transport across the sandwich. Due to the symmetry of their computational domain, interface conductance at a single Au–SAM junction can be determined to fall between 446 and 466 MW m$^{-2}$ K$^{-1}$ at 300 K.

Zhang *et al.*[14] used nonequilibrium molecular dynamics to gain further insight into the experimental work of Wang *et al.*[9,10] In this work, they found that thermal transport across Au–SAM junctions could be separated into two different temporal regimes, the first (<20 ps after flash heating of the Au substrate) in which Au atoms of the substrate and the terminal S atoms of the SAM layer reach thermal equilibrium, and the second (100–200 ps after flash heating of the Au substrate) in which Au atoms of the substrate and the alkane backbones of the molecules reach thermal equilibrium. The ultrafast sum-frequency generation (SFG). measurements of Wang *et al.*[9,10] probed transport during this first regime, whereas the measurements of Wang *et al.*,[8] as well as the simulations of Luo and Lloyd,[12,13] focused on mechanisms during the second regime.

In the present study, we have sought to offer further explanation of the observed insensitivity of solid–SAM conductance to molecule length.[14] In particular, we have investigated the vibrational spectra of alkanedithiol SAMs as a function of the number of methylene groups forming the molecular backbones of the molecules via Hartree–Fock methods, paying special attention to the vibrational overlap between the SAM and Au (a common contacting solid). It is found that despite the addition of nine new vibrational modes per added methylene group, only one "elastically accessible" mode is added. This, in combination with the changing length of the molecules within the SAM layer, can be used to explain the observed insensitivity. Furthermore, we have developed a diffusive transport model for predicting interface conductance at solid–SAM junctions, itself a loose adaptation of the widely implemented diffuse mismatch model.[15] We find an excellent agreement between the predictions of this model and the available experimental data in the literature. In addition, this model demonstrates that while many factors influence thermal interface conductance, e.g., surface roughness[16] and adhesion energy,[17] thermal transport across Au–SAM interfaces is limited by the phononic/vibrational overlap between the Au and SAM.

## II. VIBRATIONAL SPECTRA OF LINEAR MOLECULES

To begin, the vibrational spectra of linear alkanedithiols were calculated, where the molecular backbone of the alkanedithiols ranged from 5 to 15 methylene groups long. All calculations were performed using the GAUSSIAN 09 W software package. The individual molecules were initially constructed with an estimated geometry in GAUSSVIEW 5. These rough molecules were subsequently sent to GAUSSIAN for the optimization (lowest energy structure) via Hartree–Fock (HF) methods with the LANL2DZ basis. The normal modes and associated vibrational frequencies output by GAUSSIAN were used in all subsequent calculations. By distributing the output frequencies into discrete intervals (bins), we generate the spectral distribution of the vibrational modes.

Figure 1 shows the calculated spectral distribution of the vibrational modes of alkanedithiols 5 and 15 methylene groups long. Each molecule has $3N - 6$ vibrational modes, where $N$ is the number of atoms comprising the molecule.[18] These results are in agreement with the work by Segal and Nitzin.[11] While total heat capacity (in units J K$^{-1}$) is directly related to the spectral distribution of vibrational modes, the volumetric specific heat capacity (in units J K$^{-1}$ m$^{-3}$), and hence, thermal conductance, is related to the vibrational density of normal modes (DOM).[18,19] Thus,

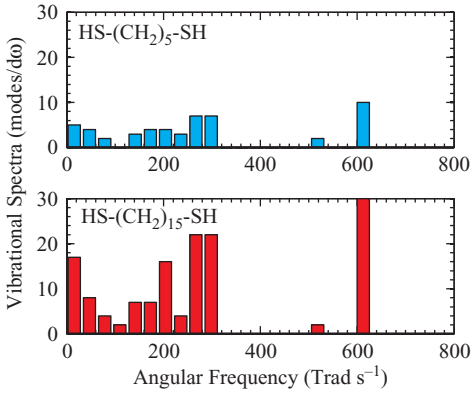


FIG. 1. Spectral distribution of the vibrational modes of alkanedithiols (top) 5 and (bottom) 15 methylene groups long calculated via Hartree–Fock methods. The total number of vibrational modes per molecule is $3N - 6$, where $N$ is the number of atoms comprising the molecule. Thus, an alkanedithiol with 5 methylene groups forming the backbone will have $3 \times 19 - 6 = 51$ modes, whereas an alkanedithiol with 15 methylene groups will have $3 \times 49 - 6 = 141$ modes, explaining the difference in the two histograms.

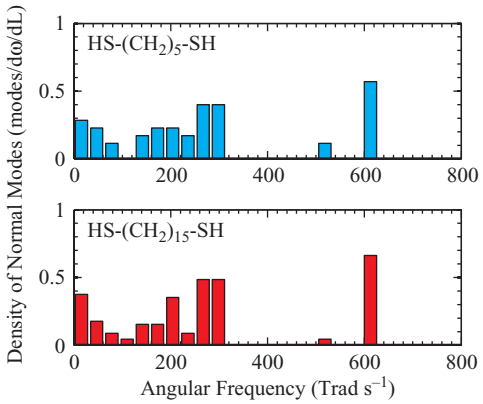


FIG. 2. The vibrational density of normal modes (number of vibrational modes per unit frequency per unit length) of alkanedithiols 5 (top) and 15 (bottom) methylene groups long. Note that despite a threefold increase in the length between HS–$(CH_2)_5$–SH and HS–$(CH_2)_{15}$–SH, the vibrational density of normal modes does not change significantly. Much of the difference between the upper and the lower plots rests in the fact that some vibrational frequencies fall very close to the edge of the bins of the histogram.

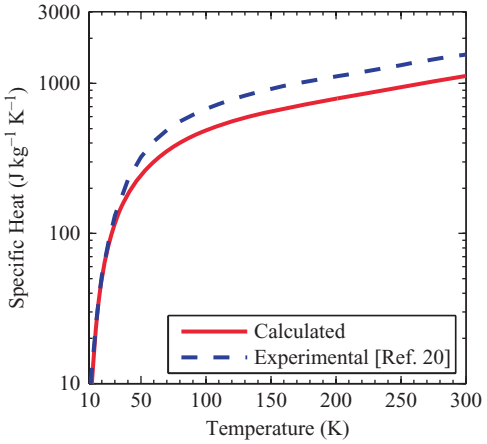


FIG. 3. Calculated specific heat capacity of octane (solid line) compared to experimental data (dashed line) from Ref. 20. Our calculations slightly underpredict experimental values. This is due to the fact that HF methods overpredict vibrational frequencies. As a result, specific heat capacity will be slightly reduced since some vibrational modes will be inaccessible as determined by the distribution function.

our remaining discussion will focus on the vibrational DOM. Figure 2 depicts the vibrational DOM of alkanedithiols 5 and 15 methylene groups long. In one-dimensional systems, the vibrational DOM is defined as the number of vibrational modes per unit energy per unit length. While each methylene group contributes nine vibrational modes to the molecule as a whole, additional methylene groups do not significantly change the vibrational DOM. In other words, molecules with more methylene groups forming their backbones have more vibrational modes, but these modes are distributed across a longer molecule. As evident in Fig. 2, the vibrational DOM does not change significantly despite the threefold increase in molecule length between HS–$(CH_2)_5$–SH and HS–$(CH_2)_{15}$–SH.

## III. VERIFICATION OF VIBRATIONAL SPECTRA

To verify the accuracy of the vibrational calculations, we once again employed the HF methods summarized above to calculate the spectral distribution of the vibrational modes of octane. With this spectral distribution in hand, we calculated the specific heat capacity of octane such that we could compare the results of our calculations to experimental thermophysical data. Specific heat capacity of a molecule, $C_p$, can be expressed as

$$C_p = \frac{1}{m}\sum_i \hbar\omega_i \frac{\partial f}{\partial T}, \tag{1}$$

where $m$ is the mass of the molecule, $\hbar$ is Planck's constant divided by $2\pi$, $\omega_i$ is the angular frequency of vibrational mode $i$, $f$ is the Bose–Einstein distribution, and $T$ is the temperature.

Figure 3 shows a comparison of our calculated heat capacity of octane compared to the heat capacity of polyethylene from Ref. 20. Polyethylene was chosen for comparison because both polyethylene and octane are linear saturated organic molecules that should have similar properties below the boiling point of octane. As clear from the plot, the agreement in trend between our calculated values and experimental values is excellent, although our calculated values are slightly below the experimental values between 50 and 300 K. This is explained by the well-known fact that HF methods traditionally overpredict vibrational frequencies.[21] As a result, specific heat capacity will be slightly reduced at lower temperatures since some vibrational modes will be inaccessible or "frozen out" as determined by the Bose–Einstein distribution function.

## IV. DIFFUSIVE TRANSPORT MODEL

In order to investigate the insensitivity of interface conductance to changes in molecule length, we have developed a diffuse phonon scattering model loosely based on the diffuse mismatch model[15] for predicting interface conductance at a solid–SAM junction. Example calculations are carried out for a Au–SAM layer such that we can compare our results directly to experimental and computational data available in the literature. The discussion of thermal transport is restricted in this context to that of phonons and molecular vibrations, as alkanedithiols are not efficient electrical conductors, and thus, electronic contributions to thermal transport are negligible.

The foundation of any diffuse scattering model requires the description of the thermal flux approaching the interface. In order to increase the accessibility while simplifying the computational requirements of the model, we employ an isotropic assumption when describing the phononic properties of Au. That is, rather than considering the full phonon dispersion across the entirety of the first Brillouin zone, we assume the isotropic dispersion based on a single direction of high crystallographic symmetry. In a previous work by the authors, it has been shown that this assumption is acceptable for predicting interface conductance across junctions between fcc crystals.[22] With respect to the present system of interest, thiol-based molecules self assemble on the (111) surface of Au.[23] Thus, we take the dispersion of Au as a fourth-order

polynomial fit of phonon dispersion from neutron scattering data along the [111] crystallographic direction.[24] With the dispersion known, the ballistic phonon flux, $q$, traversing the junction from Au to SAM can be represented as

$$q^{1\to 2} = \frac{1}{8\pi^2}\sum_j \int_{k_j} \hbar\omega_j(k_j)\, k_j^2\, \zeta^{1\to 2}\, |v_j(k_j)|\, f\, dk_j, \tag{2}$$

where $k$ is the wavevector, $\zeta$ is the transmission probability, $v$ is the phonon group velocity and equal to $\partial\omega/\partial k$, and $j$ is the polarization (e.g., longitudinal acoustic, transverse acoustic, etc.). Again, only the phonon flux of Au is considered (i.e., electronic contributions to thermal transport in Au are ignored) since the alkanedithiol SAM layer is not electrically conductive. Flux traversing the junction in the opposite direction, i.e., from SAM to Au, can be represented as

$$q^{2\to 1} = \frac{1}{A}\frac{1}{L}\sum_i \hbar\omega_i \zeta^{2\to 1} f v, \tag{3}$$

where $A$ is the coverage area per alkanedithiol and $L$ is the length of the alkanedithiol calculated from the optimized geometry. Coverage area is taken as $2.16\times 10^{-19}$ m$^2$ (from Ref. 23), and effective group velocity is assumed to be near that of polyethylene and is taken as 2300 m s$^{-1}$ (from Ref. 25). This formulation of flux in the SAM (an anisotropic media) is similar to that given by Duda *et al.*,[26] in which the authors described graphite as a linear superposition of uncoupled two-dimensional vibrational subsystems. It was found that this approach was valid due to the fact that intralayer interactions were much stronger than interlayer interactions. A similar case can be made for SAMs, where intramolecular interactions are much stronger than intermolecular interactions. When computing the flux from Au to SAM via Eq. (2), only modes that fall below the cutoff frequency of Au are considered. This "elastic" approach was chosen due to the fact that Segal and Nitzin[11] previously demonstrated anharmonicity within linear alkanes is weak, eliminating the possibility that inelastic processes at the interface will contribute to interface conductance. Furthermore, Au–Au interactions are the most "vibrationally restrictive" at the interface in the present system of interest. This has been determined by taking the second spatial derivative of empirical potentials that describe Au–Au and Au–S interactions (from Ref. 12) to determine a harmonic force constant. With this force constant and the effective mass of the oscillators known ($\sqrt{m_1 m_2}$), one can quantitatively, albeit via first approximation, compare characteristic frequencies of different bonds. The frequency associated with the Au–S bonds is roughly 30% higher than that of the Au–Au bond.

With the fluxes approaching the junction established, $\zeta^{1\to 2}$ can be determined through the application of detailed balance. In this context, the principle of detailed balance assumes the temperature drop across the interface is small,[27] and thus, $q^{1\to 2} = q^{2\to 1}$ (see Ref. 28 for a thorough assessment of this procedure). In addition, under the diffuse assumption $\zeta^{1\to 2} = 1 - \zeta^{2\to 1}$. Using this relationship and the representations of the flux approaching the interface detailed in Eqs. (2) and (3), the transmission probability is given by

$$\zeta^{1\to 2} = \frac{\frac{1}{A}\frac{1}{L}\sum_i \hbar\omega_i f v}{\frac{1}{8\pi^2}\sum_j \int_{k_j} \hbar\omega_j(k_j)\, k_j^2\, |v_j(k_j)|\, f\, dk_j + \frac{1}{A}\frac{1}{L}\sum_i \hbar\omega_i f v}. \tag{4}$$

This approach describes a scenario in which coupling between Au phonons and SAM molecular vibrations must occur within the immediate proximity of the interface. Such a treatment is warranted since, as mentioned above, anharmonicity within linear alkanes is weak,[11] and thus, inelastic coupling (analogous to three-phonon processes in crystals) along the chains is limited. In addition, this qualitative description is consistent with the experimental work of Wang *et al.*[9,10] and the computational results of Zhang *et al.*,[14] both of which demonstrated that thermal transport at Au–SAM interfaces is inherently restricted at the interface itself. With the transmission probability established, the temperature derivative of Eq. (2) yields an expression for thermal interface conductance at a Au–SAM junction, given as

$$h = \frac{1}{8\pi^2}\sum_j \int_{k_j} \hbar\omega_j(k_j)\, k_j^2\, \zeta^{1\to 2}\, |v_j(k_j)|\, \frac{\partial f}{\partial T}\, dk_j. \tag{5}$$

Through implementation of Eq. (5), we have calculated interface conductance for Au–SAM junctions where the alkanedithiols comprising the SAM ranged from 5 to 15 methylene groups long, the results of which are shown in Fig. 4.

In order to validate our model, we have selected two different experimental data sets, namely, that of Ge *et al.*[4] and Z. Wang *et al.*[9] As is apparent in Fig. 4, the predictions of our model do not line up with the data point of Ge *et al.*[4]

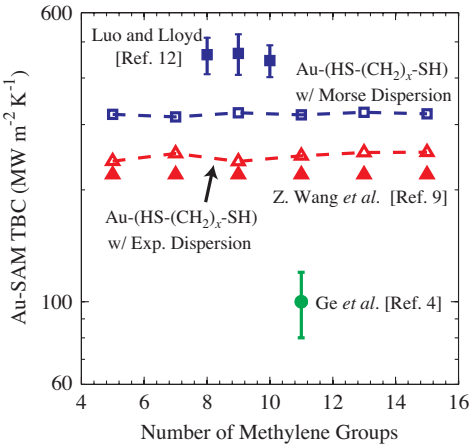


FIG. 4. Calculated (hollow symbols) interface conductance as a function of the number of methylene groups forming the backbone of the alkanedithiol compared to available experimental and computational data (filled symbols). Two different sets of Au parameters were implemented with the model to best represent the exact data to which the model predictions were compared. For comparison with the experimental data of Z. Wang *et al.*, experimental phonon dispersion was implemented. For comparison with the computational data of Luo and Lloyd, phonon dispersion was calculated via harmonic lattice dynamics with the same potential and parameters as implemented in their study. In either case, the insensitivity of interface conductance to SAM length is clear.

However, this can be explained by the fact that the "interface" examined in that work was, in fact, a composite Au-SAM-$H_2O$ junction. It is reasonable to assume that poor vibrational coupling between molecules and water lead to lower observed conductances. On the other hand, Z. Wang *et al.*[9] examined a single Au-SAM interface, thus making their data better suited for comparison to our model. From Fig. 4, the predictions of our model are in excellent agreement with their data, both in observed values and trends.

On the other hand, we found the present model underpredicted the previously established computational results of Ref. 12, which considered interface conductance at Au–alkanedithiol interfaces. However, in Ref. 12, Au–Au interactions were described by the Morse potential. To determine the degree to which this change in the description of Au would effect the predictions of the present model, we employed the General Utility Lattice Program (GULP) software package[29] to calculate phonon dispersion of Au using the Morse potential with the same parameters as those used in Ref. 12 ($D_e = 0.475$ eV, $a = 1.583$ Å$^{-1}$, and $r_0 = 3.0242$ Å, all taken from Ref. 30). We found that the Morse potential implemented in Ref. 12 yields significantly greater ($\sim$50%) maximum phonon frequencies and group velocities than those determined experimentally. The present model is sensitive to the description of phonon frequencies and group velocities of Au (Eq. (5) scales with group velocity). Thus, when implementing the calculated Morse phonon dispersion of Au (rather than experimental) in the present model, we find a better agreement between the predictions of our model and the computational data.

It is important to note that, although our model is quantum mechanical and not classical (since we rely on the Bose–Einstein distribution to describe the occupancy of the respective vibrational DOM of Au and the SAM), we can still compare the predictions of this model to the classical MD results from Ref. 12. This is due to the fact that the Debye temperature of Au is 170 K (from Ref. 19) and the simulations were performed at 300 K. Thus, at this temperature, Au behaves classically. While the simulated temperature is not above the Debye temperature of the SAM, the harmonicity of the SAM prevents inelastic phonon–phonon interactions from occurring within the SAM itself. Thus, the vibrational modes responsible for transport across the Au–SAM interface are subject to the distribution of modes in the Au substrate.

In order to explain the insensitivity of interface conductance to molecule length seen in Fig. 4, we return to the results presented in Fig. 2. As discussed above, in terms of the vibrational DOM (number of modes per unit frequency per unit length), the additional modes that result from increasing the number of methylene groups along the molecule backbones are negated by the increasing molecule length. Consequently, Eq. (3) will predict nearly the same flux regardless of the number of methylene groups comprising the same. This is due to the fact that the flux approaching the interface is directly related to the vibrational DOM. In turn, the transmission probability which ultimately governs interface conductance remains unchanged, leading to a nearly constant interface conductance.

## V. CONCLUSION

We have investigated the vibrational spectra of alkanedithiol-based SAMs as a function of the number of methylene groups forming the molecular backbone via Hartree–Fock methods. These spectra were used as an input into a diffusive transport model to predict interface conductance at solid–SAM junctions. We have shown that the predictions of this model are in an excellent agreement with previous experimental and computational data of interface conductance at Au–alkanedithiol junctions. Through consideration of the vibrational density of normal modes, we explain the observed insensitivity of interface conductance to the number of methylene groups forming the molecular backbones. It is shown that despite the addition of nine vibrational modes per methylene group, the one-dimensional density of normal modes remains nearly unchanged. This model demonstrates that while many factors influence thermal interface conductance, thermal transport across Au–SAM interfaces is limited by the phononic/vibrational overlap between the Au and SAM.

## ACKNOWLDGMENTS

J.C.D. is appreciative for funding from the National Science Foundation Graduate Research Fellowship Program. C.B.S. is appreciative for funding from U.Va. through the form of a Commonwealth Fellowship, as well as C. O. Trindle at U.Va. for his insightful discussions regarding the density of quantum states. P.E.H. is appreciative for funding from the LDRD program office through the Sandia National Laboratories Harry S. Truman Fellowship Program. Sandia is a multiprogram laboratory operated by Sandia Corporation, a wholly owned subsidiary of Lockheed Martin Corporation, for the United States Department of Energy's National Nuclear Security Administration under Contract DE-AC04-94AL85000.

[1] M. A. Reed, Proc. IEEE **87**, 652 (1999).
[2] P. Reddy, S.-Y. Jang, R. A. Segalman, and A. Majumdar, Science **315**, 1568 (2007).
[3] O. M. Wilson, X. Hu, D. G. Cahill, and P. V. Braun, Phys. Rev. B **66**, 224301 (2002).
[4] Z. Ge, D. G. Cahill, and P. V. Braun, Phys. Rev. Lett. **96**, 186101 (2006).
[5] M. Hu, J. V. Goicochea, B. Michel, and D. Poulikakos, Appl. Phys. Lett. **95**, 51903 (2009).
[6] D. Segal and A. Nitzan, J. Chem. Phys. **122**, 94704 (2005).
[7] D. Segal and A. Nitzan, J. Chem. Phys. **117**, 3915 (2002).
[8] R. Y. Wang, R. A. Segalman, and A. Majumdar, Appl. Phys. Lett. **89**, 173113 (2006).
[9] Z. Wang, J. A. Carter, A. Lagutchev, Y. K. Koh, N.-H. Seong, D. G. Cahill, and D. D. Dlott, Science **317**, 787 (2007).
[10] Z. Wang, D. G. Cahill, J. A. Carter, Y. K. Koh, A. Lagutchev, N.-H. Seong, and D. D. Dlott, Chem. Phys. **350**, 31 (2008).
[11] D. Segal, A. Nitzan, and P. Hänggi, J. Chem. Phys. **119**, 6840 (2003).
[12] T. Luo and J. R. Lloyd, J. Heat Transfer **132**, 32401 (2010).
[13] T. Luo and J. R. Lloyd, Int. J. Heat Mass Transfer **53**, 1 (2010).
[14] Y. Zhang, G. L. Barnes, T. Yan, and W. L. Hase, Phys. Chem. Chem. Phys. **12**, 4435 (2010).
[15] E. T. Swartz and R. O. Pohl, Rev. Mod. Phys. **61**, 605 (1989).
[16] P. E. Hopkins, L. M. Phinney, J. R. Serrano, and T. E. Beechem, Phys. Rev. B **82**, 085307 (2010).
[17] R. Prasher, Appl. Phys. Lett. **94**, 041905 (2009).
[18] G. Chen, *Nanoscale Energy Transport and Conversion: A Parallel Treatment of Electrons, Molecules, Phonons, and Photons* (Oxford University Press, New York, 2005).

[19]N. W. Ashcroft and N. D. Mermin, *Solid State Physics* (Thomson Learning, 1976).
[20]U. Guar and B. Wunderlich, J. Phys. Chem. Ref. Data **10**, 119 (1981).
[21]M. D. Halls, J. Velkovski, and H. B. Schlegel, Theor. Chem. Acc. **105**, 413 (2001).
[22]J. C. Duda, T. E. Beechem, J. L. Smoyer, P. M. Norris, and P. E. Hopkins, J. Appl. Phys. **108**, 073515 (2010).
[23]F. Schreiber, Prog. Surf. Sci. **65**, 151 (2000).
[24]J. W. Lynn, H. G. Smith, and R. M. Nicklow, Phys. Rev. B **8**, 3493 (1973).
[25]D. V. Krevelen, *Properties of Polymers*, 4th ed. (Elsevier, Amsterdam, 2009).
[26]J. C. Duda, J. L. Smoyer, P. M. Norris, and P. E. Hopkins, Appl. Phys. Lett. **95**, 031912 (2009).
[27]While this assumption is not valid in the case of ultrafast flash heating of the Au substrate as described in Refs. 9, 10, 14, it is valid in the case of moderate heating schemes where applied thermal fluxes are low.
[28]J. C. Duda, P. E. Hopkins, J. L. Smoyer, M. L. Bauer, T. E. English, C. B. Saltonstall, and P. M. Norris, Nanoscale Microscale Thermophys. Eng. **14**, 21 (2010).
[29]J. D. Gale and A. L. Rohl, Mol. Simul. **29**, 291 (2003).
[30]R. C. Lincoln, K. M. Koliwad, and P. B. Ghate, Phys. Rev. **157**, 463 (1967).